AD-756 662

Experimental Investigation into a Commutative Filter

Naval Missile Center

MARCH 1973

Technical Publication TP-73-7

EXPERIMENTAL INVESTIGATION INTO A COMMUTATIVE FILTER

By

M. L. RYKEN, JR.
Electronic Warfare Division

6 March 1973

NAVAL MISSILE CENTER

Point Mugu, California

TP-73-7 (U)

40
R

NAVAL MISSILE CENTER

AN ACTIVITY OF THE NAVAL AIR SYSTEMS COMMAND

E. E. IRISH, CAPT USN
Commanding Officer

The thesis reprinted in this report was written by Mr. M. L. Ryken, Jr., in partial fulfillment of the requirements for his master's degree in engineering at the University of California, Los Angeles.

Mr. T. Kitabayashi, Head, Design and Development Branch, and Mr. L. V. Thompson, Head, Electronic Warfare Division, have reviewed this report for publication.

Technical Publication TP-73-7

Published by . . . . . Editing and Writing Branch
Technical Publications Division
Photo/Graphics Department
Security classification . . . . . UNCLASSIFIED
First printing . . . . . 60 copies

UNCLASSIFIED

Security Classification

DOCUMENT CONTROL DATA - R & D

(Security classification of title, body of abstract and indexing annotation must be entered when the overall report is classified)

1. ORIGINATING ACTIVITY (Corporate author)	2a. REPORT SECURITY CLASSIFICATION
Naval Missile Center Point Mugu, California 93042	UNCLASSIFIED
	2b. GROUP

3. REPORT TITLE

EXPERIMENTAL INVESTIGATION INTO A COMMUTATIVE FILTER

4. DESCRIPTIVE NOTES *(Type of report and inclusive dates)*

5. AUTHOR(S) *(First name, middle initial, last name)*

Marvin L. Ryken, Jr.

6. REPORT DATE	7a. TOTAL NO. OF PAGES	7b. NO. OF REFS
6 March 1973	~~38~~ 40	10

8a. CONTRACT OR GRANT NO.	9a. ORIGINATOR'S REPORT NUMBER(S)
b. PROJECT NO.	TP-73-7
c.	9b. OTHER REPORT NO(S) *(Any other numbers that may be assigned this report)*
d.	

10. DISTRIBUTION STATEMENT

Approved for public release; distribution unlimited.

11. SUPPLEMENTARY NOTES	12. SPONSORING MILITARY ACTIVITY
	Naval Air Systems Command

13. ABSTRACT

A commutative filter is a bandpass filter capable of very high Q's, large range of resonant frequency (0 to 2 megahertz that can be electronically tuned), comb-filter frequency response, small bandwidth (independent of resonant frequency), and extremely small size (can be constructed of integrated circuits since no inductors are required). These are some of the advantages of the commutative filter.

The purpose of ~~this paper~~ is to present the general theory and evaluation of a commutative filter, in which presentation the effects of "leaky" capacitors and load resistance are considered. An eight-channel filter is built, and laboratory and theoretical results are compared for the transfer function, bandwidth, quality factor, and sensitivity of the commutative filter. The commutative filter is also investigated from the viewpoint of enhancement of signal-to-noise ratio.

DD FORM 1 NOV 65 1473 (PAGE 1)

S/N 0101-807-6801

UNCLASSIFIED

Security Classification

14 KEY WORDS	LINK A		LINK B		LINK C	
	ROLE	WT	ROLE	WT	ROLE	WT
Bandpass filters Commutative filters Digital filters Electronic countermeasures equipment						

CONTENTS

Page

SUMMARY 1

SYMBOLS 3

Chapter

I COMMUTATIVE FILTER THEORY 5
- 1.1 Introduction 5
- 1.2 Transfer Function 6
- 1.3 Bandwidth and Q 11
- 1.4 Sensitivity 13
- 1.5 Signal-to-Noise Improvement 15

II PRACTICAL REALIZATION OF A COMMUTATIVE FILTER 17
- 2.1 Filter Design 17
- 2.2 Evaluation of Commutative Filter 20
  - 2.2.1 Transfer Function Evaluation 21
  - 2.2.2 Bandwidth and Q Evaluation 22
  - 2.2.3 Sensitivity Evaluation 26
  - 2.2.4 Signal-to-Noise Improvement Evaluation 26

III DISCUSSION OF RESULTS 31
- 3.1 Transfer Function 31
- 3.2 Bandwidth and Q 31
- 3.3 Sensitivity 32
- 3.4 Signal-to-Noise Improvement 32

IV CONCLUSION 33

BIBLIOGRAPHY 35

TABLES
1. Values of Commutative Filter Sensitivities 27
2. S/N Improvement Factor, I, of the Commutative Filter 30

CONTENTS (Concluded)

Page

FIGURES

1. Schematic Diagram of the Bandpass Commutative Filter 6
2. Equivalent Circuit for One Channel of the Filter During the Charging Cycle 7
3. Thevenin's Equivalent Circuit of the Circuit in Figure 2 7
4. Schematic Diagram of One Channel of the Filter During the Noncharging Time 7
5. Waveform Across the n^{th} Capacitor 8
6. Bandpass Characteristic of Output of Commutative Filter 13
7. Pulse Train 15
8. Frequency Spectrum of Pulse Train for $T_p/T = 0.167$ Where $w = 2\pi/T$ . . . 15
9. Filter Circuit Diagram 18
10. Logic Circuit Diagram 19
11. Logic Waveforms and Logic Truth Table 20
12. Block Diagram for Determining Attenuation at Resonant and Harmonic Frequencies 21
13. Resonant Frequency and Harmonic Output Response 22
14. Block Diagram for Obtaining Frequency Plots of the Commutative Filter 23
15. Schematic Diagram for the Voltage Ramp Generator 23
16. Frequency Response of Commutative Filter at f_r = 1.25 Kilohertz 24
17. Center Frequency Response at f_r = 125 Hertz 24
18. Center Frequency Response With Constant BW for Varied f_r 25
19. Center Frequency Response When R_2 Is Varied 25
20. Center Frequency Response for R_c Varied 26
21. Sensitivity of Center Frequency Response to Small Changes in C 28
22. Sensitivity of Center Frequency Response to Small Changes in R_1 28
23. Block Diagram for Obtaining S/N Improvement Factor 29
24. Mixer Circuit Diagram 29

TP-73-7
6 March 1973

NAVAL MISSILE CENTER
Point Mugu, California

EXPERIMENTAL INVESTIGATION INTO A COMMUTATIVE FILTER

By
M. L. RYKEN, JR.

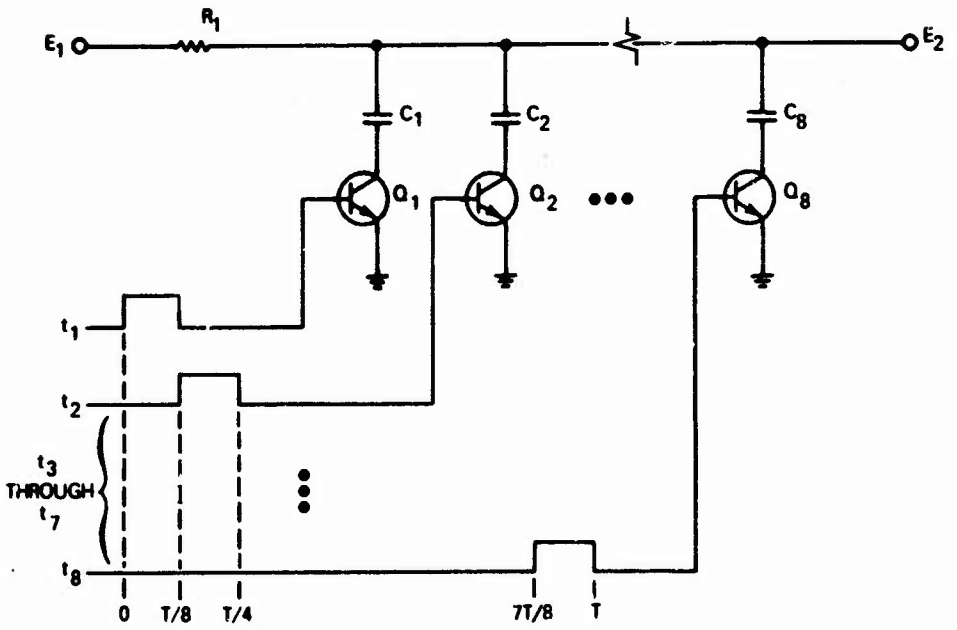

SUMMARY

A commutative filter is a bandpass filter capable of very high Q's, large range of resonant frequency (0 to 2 megahertz) that can be electronically tuned, comb-filter frequency response, small bandwidth (independent of resonant frequency), and extremely small size (can be constructed of integrated circuits since no inductors are required). These are some of the advantages of the commutative filter.

The purpose of this paper is to present the general theory and evaluation of a commutative filter; the effects of "leaky" capacitors and load resistance are considered. An eight-channel filter is built, and laboratory and theoretical results are compared for the transfer function, bandwidth, quality factor, and sensitivity of the commutative filter. The commutative filter is also investigated from the viewpoint of enhancement of signal-to-noise ratio.

SYMBOLS

A – Amplitude weighting factor

BW – 3-decibel bandwidth

C – Capacitor

$e_I(t)$ – Instantaneous input voltage

$e_e(t)$ – Equivalent instantaneous input voltage

$e_n(t)$ – Instantaneous voltage across the n *th* capacitor

$e_n(ss)$ – Steady-state voltage across the n *th* capacitor

F(f) – Transfer function

f – Frequency

f_r – Resonant frequency of filter/commutator rotation rate

f_{3dB} – Frequency when F(f) is down 3 decibels

H(w) – Frequency response function

I – Signal-to-noise improvement factor

Im – Imaginary part

N – Number of capacitor channels

N_i – Input noise

N_o – Output noise

N(f) – Input noise average power per cycle

Q – Quality factor

R_1 – Input resistor

R_2 – Load resistor

R_c – Capacitance leakage resistor

R_e – Equivalent charging resistance

R_p – Equals $R_c/R_e + N-1$

S/N – Signal-to-noise

$S_x^{F(x)}$ – Sensitivity of $F(x)$ to changes in x

T_d – Charging time/dwell time

T_r – Time between samples/period of one rotation

t_T – Equals $T_d/R_eC - (N-1)T_d/R_cC$

w – Frequency in radians per second

Chapter I

COMMUTATIVE FILTER THEORY

1.1 Introduction

The recent interest in commutative filters results from the present lack of high-quality inductors for integrated-circuit bandpass filters. The present solution for the lack of inductors has been to use RC (resistance-capacitance) active filters. The problem with this technique is that the RC active filter is very sensitive to amplifier gain. It has been shown[1] that for a twin-tee feedback network, the sensitivity of the Q (quality factor) of the filter to changes in amplifier gain is equal to two times the value of the Q. So for a high-Q filter, changes in the amplifier gain will result in large changes in the filter's characteristics. This is not the case with the commutative filter. The commutative filter's sensitivity depends on the clock frequency stability and the RC low-pass sections as will be demonstrated later. The commutative filter also has some interesting properties, one being a comb-filter frequency response.

Figure 1 is the schematic diagram for a bandpass commutative filter. The resistor R_1 and a capacitor C_i (where i = 1, 2, 3, . . . , or N) make up one low-pass RC filter channel where there are N channels. The value of all the capacitors are equal and of value C. The resistor R_2 is the load resistance. The commutator rotates at a constant frequency, f_r. The contacts are closed for the dwell time, T_d, where

$$T_d = T_r/N \tag{1}$$

and the commutator period, T_r, is defined as

$$T_r = 1/f_r \tag{2}$$

This assumes no dead time between contacts and that no more than one contact is connected at a time. The value of R_2 should be much larger than the value of R_1 and the low-pass filter time constant, R_1C, should be larger than the dwell time, T_d, for the best filter characteristics, as will be demonstrated later.

[1] James Thompson, "RC Digital Filter For Microcircuit Bandpass Amplifiers," Electronic Equipment Engineering, V.108 (March, 1964), p. 45.

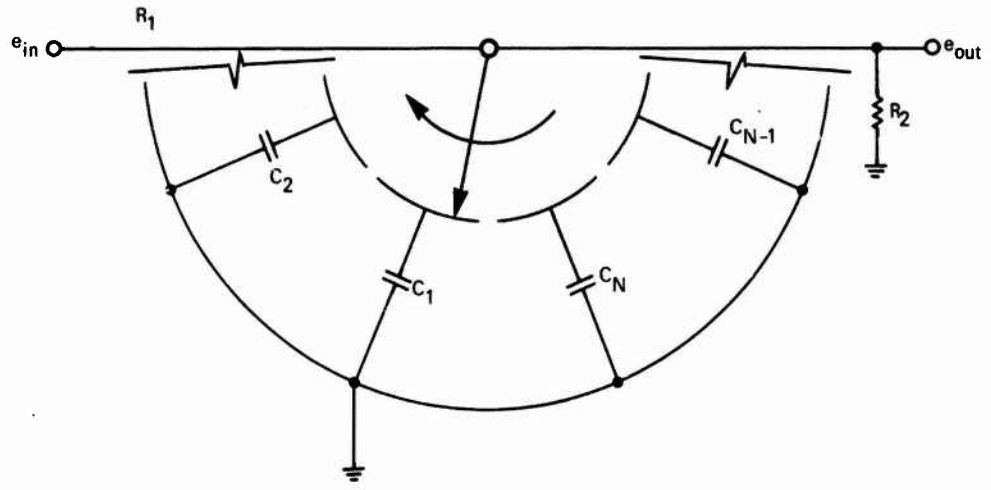

Figure 1. Schematic Diagram of the Bandpass Commutative Filter.

Becausc of the commutator action, each capacitor becomes exposed successively to a segment of the input signal. The voltage across each capacitor is then charged to the average value of its segment of the input voltage. The charging rate of the voltage onto the capacitor is governed by the R_1C time constant. Since the R_1C time constant is larger than the dwell time, T_d, it will take several revolutions of the commutator before the capacitor can be charged to the average value of the segment of the input voltage. Therefore if the input signal frequency is synchronous (a frequency equal to f_r or one of its harmonics) to the commutator rotation frequency, f_r, the average value of the segment will ultimately appear on the capacitor. This value is neglecting the loading effect of R_2 since it was assumed that the value of R_2 was much greater than the value of R_1. But if the input signal frequency is not synchronous to the commutator rotation frequency, the average value of the segment of the input voltage will be different for each revolution of the commutator. The capacitor will charge to a small voltage close to zero since the average value of the segment of the input voltage changes for each revolution. This sequence is the principle of operation of the commutative filter.

For a synchronous frequency sine-wave input, the output will look like a sampled sine wave. Postfiltering will then be needed if the input sine-wave form is to be reconstructed.

1.2 Transfer Function

The transfer function will be calculated for the most general case where "leaky capacitors" and a load resistor will be considered. The "leaky capacitors" will be represented by the capacitor C in parallel with a resistor of value R_c. The load resistor is R_2. The charging cycle (when the commutator switch is closed) for one channel of the filter is shown in figure 2. This diagram can be reduced by Thevenin's theorem to the circuit shown in figure 3.

$$R_e = \frac{R_1R_2R_c}{R_1R_2 + R_cR_1 + R_2R_c} \tag{3}$$

and

$$e_e = \frac{e_1 R_2 R_c}{R_1 R_2 + R_c R_1 + R_2 R_c} = e_1 \frac{R_e}{R_1} \qquad (4)$$

For the charging period, T_d, the capacitor charges with a $R_e C$ time constant. The noncharging time, $(N-1)T_d$, of the circuit for one channel is shown in figure 4.

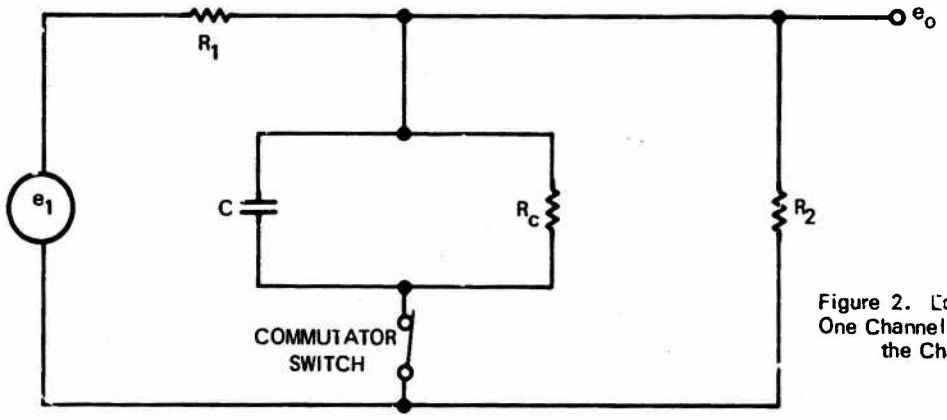

Figure 2. Equivalent Circuit for One Channel of the Filter During the Charging Cycle.

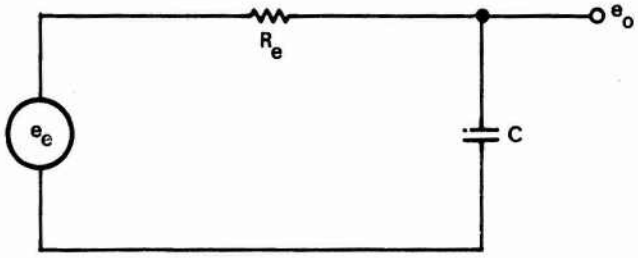

Figure 3. Thevenin's Equivalent Circuit of the Circuit in Figure 2.

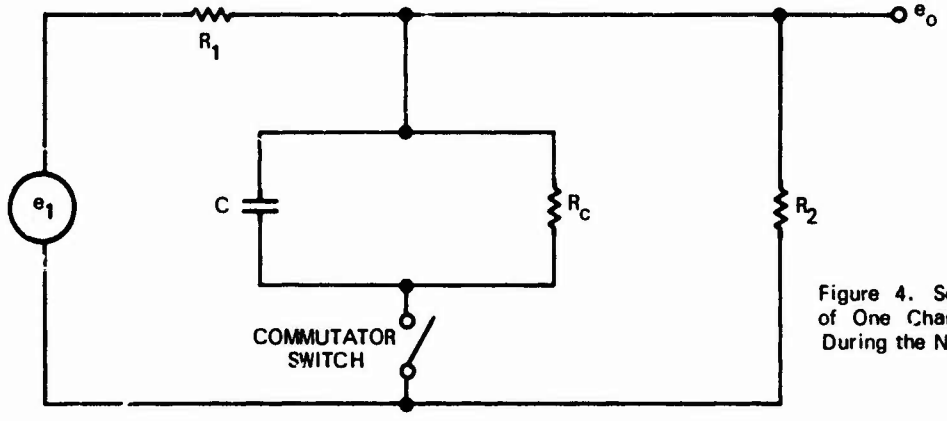

Figure 4. Schematic Diagram of One Channel of the Filter During the Noncharging Time.

Figure 5 shows the waveform across this capacitor for one period of rotation $\left(T_r = NT_d\right)$ where e_n is the voltage across the n*th* capacitor.

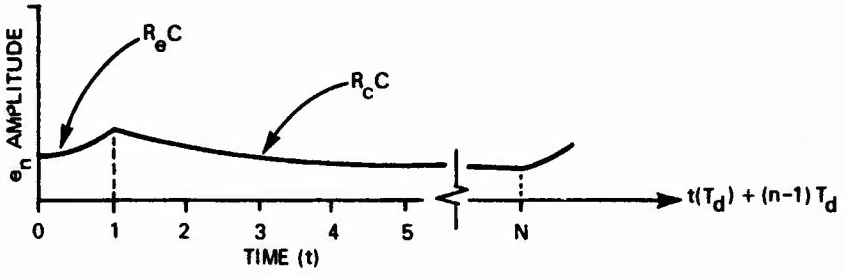

Figure 5. Waveform Across the n^{th} Capacitor.

The voltage source input to the n*th* channel at the end of the (k + 1) charging cycle can be expressed as:

$$e_1 = e_1\left(nT_d + kT_r\right) \tag{5}$$

The voltage across the n*th* capacitor at the end of its k*th* charging cycle is

$$e_n = e_n\left[nT_d + (k-1)T_r\right] \tag{6}$$

The voltage across the n*th* capacitor at the beginning of the (k + 1) charging cycle is

$$e_n = e_n\left[nT_d + (k-1)\,T_r\right]\, e^{-(N-1)T_d/R_cC} \tag{7}$$

The difference between the voltages in equations 6 and 7 is due to the discharge of the capacitor through R_c. The voltage across the n*th* capacitor at the end of the (k + 1) charging period will then be

$$e_n\left(nT_d + kT_r\right) = e_n\left[nT_d + (k-1)T_r\right] e^{-(N-1)T_d/R_cC + T_d/R_eC}$$

$$+\frac{R_e}{R_1}\, e_1\left(nT_d + kT_r\right)\left(1-e^{-T_d/R_eC}\right) \tag{8}$$

Similar equations can be written for the n*th* capacitor during the k*th* down to the 0*th* charging period. If these equations are substituted into equation 8 the following series will result for the voltage across the n*th* capacitor at the end of the (k + 1) charging period.

$$e_n\left(nT_d + kT_r\right) = \left(1-e^{-T_d/R_eC}\right)\frac{R_e}{R_1}\sum_{r=0}^{k} e^{-r\left(\frac{T_d}{R_eC} + \frac{(N-1)T_d}{R_cC}\right)} \cdot e_1\left[nT_d + (k-r)T_r\right] \tag{9}$$

If the input, e_1, is assumed a sine wave where

$$e_1 = E \sin 2\pi ft = E \text{ Im } e^{j2\pi ft},$$

then

$$e_1\left[nT_d + (k-r)T_r\right] = E \text{ Im } e^{j2\pi f\left[nT_d + (k-r)T_r\right]} \tag{10}$$

Substituting this in equation 9 yields

$$e_n\left(nT_d + kT_r\right) = \frac{ER_e}{R_1}\left(1-e^{-T_d/R_eC}\right)\text{Im}\left[e^{j2\pi f\left(nT_d + kT_r\right)}\right.$$

$$\left.\cdot\sum_{r=o}^{k} e^{-r\left(\frac{T_d}{R_eC} + \frac{(N-1)T_d}{R_cC} + j2\pi fT_r\right)}\right] \tag{11}$$

The steady-state voltage across the *nth* capacitor is then obtained by letting k approach a large number in equation 11. The resulting equation is

$$e_n(ss) = \frac{ER_e}{R_1}\left(1-e^{-T_d/R_eC}\right)\text{Im}\left[e^{j2\pi f\left(nT_d + kT_r\right)}\right.$$

$$\left.\cdot\frac{1}{1-e^{-\left(\frac{T_d}{R_eC} + \frac{(N-1)T_d}{R_cC} + j2\pi fT_r\right)}}\right] \tag{12}$$

The transfer function for the steady-state condition is given by:

$$F(f) = \frac{e_n(ss)}{e_1} = \left(1-e^{-T_d/R_eC}\right)\frac{R_e}{R_1}$$

$$\cdot \text{Im}\,\frac{1}{1-e^{-\left(\frac{T_d}{R_eC} + \frac{(N-1)T_d}{R_cC} + 2\pi fT_r\right)}} \tag{13}$$

By substitution of $e^{-2\pi f T_r} = \cos 2\pi f/f_r - j\sin 2\pi f/f_r$ into equation 13, the magnitude of the transfer function is[2]

$$|F(f)| = \frac{R_e}{R_1} \frac{1-e^{-T_d/R_eC}}{1-e^{-\left[T_d/R_eC + (N-1)T_d/R_cC\right]}} \cdot \frac{1}{\sqrt{1+\frac{2e^{-T_d/R_eC + (N-1)T_d/R_cC}}{\left[1-e^{-\left(T_d/R_eC + (N-1)T_d/R_cC\right)}\right]^2}\left(1-\cos\frac{2\pi f}{f_r}\right)}} \tag{14}$$

If the time constant R_eC is larger than T_d and if the time constant R_cC is larger than $(N-1)T_d$, then

$$e^{-T_d/R_eC} \cong 1 - T_d/R_eC \tag{15}$$

and

$$e^{-\left[T_d/R_eC + (N-1)T_d/R_cC\right]} \cong 1 - \left[T_d/R_eC + (N-1)T_d/R_cC\right] \tag{16}$$

The transfer function then reduces to

$$|F(f)| = \frac{R_e^2R_c}{R_1\left[R_c + (N-1)R_e\right]} \cdot \frac{1}{\left[1 + \frac{2\left[1-T_d/R_eC - (N-1)T_d/R_cC\right]}{\left[T_d/R_eC + (N-1)T_d/R_cC\right]^2}\left(1-\cos\frac{2\pi f}{f_r}\right)\right]^{1/2}} \tag{17}$$

At the resonant frequency ($f = nf_r$ where $n = 0, 1, 2, \ldots, N$)

$$|F(f_r)| = \frac{R_e^2R_c}{R_1\left[R_c + (N-1)R_e\right]} \tag{18}$$

[2]A.R. Dabrowa, "Analysis of Commutated Filter" UCLA Master of Science in Engineering Thesis, 1967, p. 15.

Minimum transfer occurs at $f = f_r/2$ where $\cos 2\pi f/f_r = -1$; therefore

$$\left|F\left(\frac{f_r}{2}\right)\right| = \frac{R_e^2 R_c}{R_1\left[R_e + (N-1)R_e\right]} \cdot \frac{1}{\left[1 + \frac{4\left[1-T_d/R_eC - (N-1)T_d/R_cC\right]}{\left[T_d/R_eC + (N-1)T_d/R_cC\right]^2}\right]^{1/2}} \tag{19}$$

The spectrum of infinitely short time-duration sampling pulse train extends to infinity. When the sampling pulse is of finite width and of rectangular shape as the output from the commutative bandpass filter, the spectrum envelope takes the shape of a (sin x)/x function.[3] Therefore, the transfer function developed should have an amplitude weighting factor, A, of

$$A = \frac{\sin \frac{n\pi}{N}}{\frac{n\pi}{N}} \tag{20}$$

Neglecting the effect of the load resistor and leaky capacitor, Thompson develops the following expression for the transfer function for the bandpass commutative filter.[4]

$$F(f) = \left[\frac{\sin \frac{n\pi}{N}}{\frac{n\pi}{N}}\right]^2 \left[\frac{1}{jNR_1C(2\pi f - 2\pi f_r) + 1} + \frac{1}{jNR_1C(2\pi f + 2\pi f_r) + 1}\right] \tag{21}$$

1.3 Bandwidth and Q

The 3-decibel frequency response of the transfer function from equation 14 where loading is included is given by:

$$1 = \frac{2e^{-\left[T_d/R_eC + (N-1)T_d/R_cC\right]}}{\left[1-e^{-\left[T_d/R_eC + (N-1)T_d/R_cC\right]}\right]^2}\left(1-\cos\frac{2\pi f}{f_r}\right) \tag{22}$$

[3] Ibid., p. 3.

[4] Thompson, op. cit., p. 49.

From this equation, if one considers the effect of the leaky capacitance and load resistance, the BW (bandwidth) is[5]

$$BW = \frac{1}{\pi N R_e C} \frac{1 + (N-1)R_e/R_c}{1 - \frac{1}{2}\left[T_d/R_eC + (N-1)T_d/R_cC\right]} \tag{23}$$

The assumption is that

$$R_eC > T_d$$

$$R_cC > (N-1)T_d$$

$$f - f_r \ll f_r$$

The Q for the filter, if one considers the effect of the leaky capacitor and load resistance, is

$$Q = \frac{f_r}{BW} = f_r \pi N R_e C \frac{1 - \frac{1}{2}\left[T_d/R_eC + (N-1)T_d/R_cC\right]}{1 + (N-1)R_e/R_c} \tag{24}$$

From equation 21 for the unloaded filter, it is obvious that the center frequency of the filter is equal to the commutator frequency of rotation, f_r. Rearranging one of the fractions in equation 21 yields

$$\frac{1}{jNR_1C(2\pi f - 2\pi f_r)} = \frac{1/2\pi NR_1C}{j(f - f_r) + 1/2\pi NR_1C} \tag{25}$$

From this expression and in reference to figure 6, it is seen that if the effects of loading are neglected, the filter bandwidth is

$$BW = \frac{1}{2\pi NR_1C}(2) = \frac{1}{\pi NR_1C} \tag{26}$$

The value of Q when the leaky capacitance and load resistance are neglected is

$$Q = \frac{f_r}{BW} = \pi f_r NR_1C \tag{27}$$

[5]Dabrowa, op. cit., p. 18.

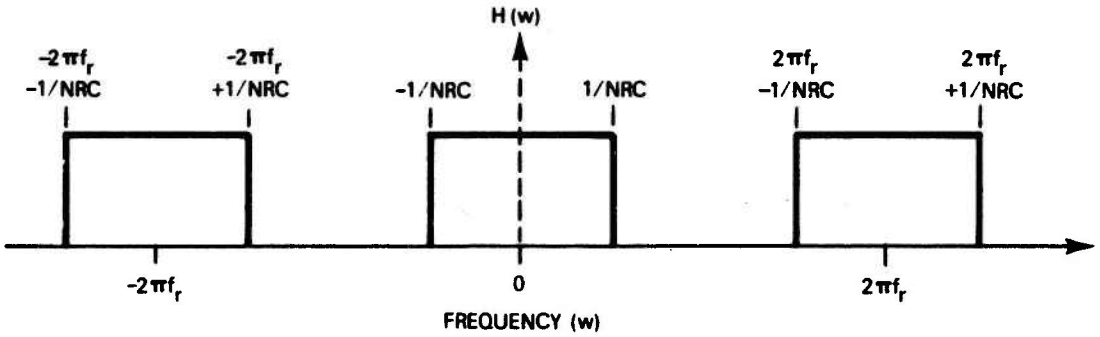

Figure 6. Bandpass Characteristic of Output of Commutative Filter.

1.4 Sensitivity

The sensitivity factor is defined by:

$$S_x^{F(x)} = \frac{\partial F(x)/F(x)}{\partial x/x} \tag{28}$$

As one can see, this relates percentage change in F(x), a function of x, to percentage change in x. Therefore the smaller the sensitivity factor the better.

The sensitivities for the commutative filter, if one considers the effects of the leaky capacitor and the load resistor, are:

$$S_{R_1}^{BW} = \frac{-1}{\frac{R_p R_1}{R_c}\left(1 - \tfrac{1}{2}t_T\right)} \tag{29}$$

$$S_{R_2}^{BW} = \frac{-1}{\frac{R_p R_2}{R_c}\left(1 - \tfrac{1}{2}t_T\right)} \tag{30}$$

$$S_{R_c}^{BW} = \frac{-1}{\frac{R_p}{N}\left(1 - \tfrac{1}{2}t_T\right)} \tag{31}$$

$$S_C^{BW} = \frac{-1}{1 - \tfrac{1}{2}t_T} \tag{32}$$

$$S_{f_r}^{BW} = \frac{-1}{1 - \tfrac{1}{2}t_T} \tag{33}$$

$$S_{R_1}^{Q} = \frac{+1}{\frac{R_p R_1}{R_c}\left(1 - \tfrac{1}{2}t_T\right)} \tag{34}$$

$$S_{R_2}^{Q} = \frac{+1}{\frac{R_p R_2}{R_c}\left(1 - \tfrac{1}{2}t_T\right)} \tag{35}$$

$$S_{R_c}^{Q} = \frac{+1}{\frac{R_p}{N}\left(1 - \tfrac{1}{2}t_T\right)} \tag{36}$$

$$S_{C}^{Q} = \frac{+1}{1 - \tfrac{1}{2}t_T} \tag{37}$$

$$S_{f_r}^{Q} = \frac{+1}{1 - \tfrac{1}{2}t_T} \tag{38}$$

where

$$t_T = \frac{T_d}{R_e C} + \frac{(N-1)r_d}{R_c R} \tag{39}$$

and

$$R_p = R_c/R_e + N - 1 \tag{40}$$

The following values of sensitivities are obtained for the commutative filter when the loading effects of the leaky capacitor and the load resistor are not considered:

$$S_{R_1}^{BW} = -1 \tag{41}$$

$$S_{C}^{BW} = -1 \tag{42}$$

$$S_{f_r}^{BW} = 0 \tag{43}$$

$$S_{R_1}^{Q} = 1 \tag{44}$$

$$S_{C}^{Q} = 1 \tag{45}$$

$$S_{f_r}^{Q} = 1 \tag{46}$$

For a good commutative filter, R_2 and R_c will be much larger than R_1, R_eC more than T_d, and R_cC more than $(N-1)T_d$. The sensitivity factors for a good commutative filter will then approach those sensitivity factors given for the unloaded filter.

1.5 Signal-to-Noise Improvement

The comb-filter response of the commutative filter can be used to good advantage in increasing the S/N (signal-to-noise) of a signal when the signal energy is concentrated at harmonics of the commutator frequency. This is accomplished by reducing the N (noise level) by filtering the noise energy out of the frequency spectrum input between the harmonics of the signal.

A pulse train has its energy concentrated at the pulse frequency and harmonics. For the pulse train in figure 7, the pulse train signal can be expressed by Fourier series expansion as:

$$f(t) = \frac{1}{\pi} \sum_{n=-\infty}^{\infty} \frac{1}{n} \sin(n\pi T_p/T)\, e^{\frac{jn2\pi}{t}(t - \frac{1}{2}T_p)} \qquad (47)$$

where T is the pulse repetition period and T_p is the pulse width. Figure 8 is an energy versus frequency plot of the pulse train when $T_p/T = 0.167$ where $w = 2\pi/T$. From figure 8 it is seen that the majority of the pulse's energy lies below the fourth harmonic of the pulse frequency where the pulse frequency equals 1/T. Therefore a commutative filter with resonant frequency equaling the pulse frequency will pass the pulse train without much attenuation or loss of the pulse waveform.

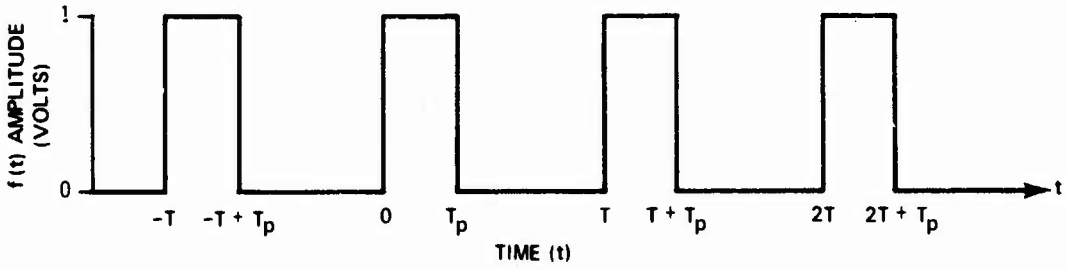

Figure 7. Pulse Train.

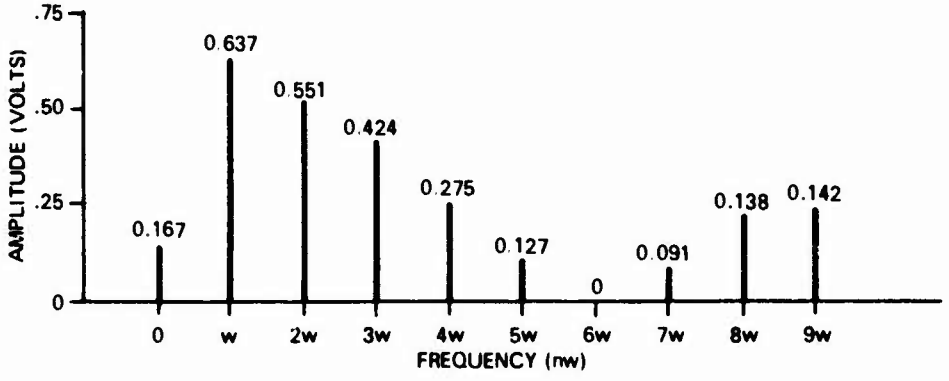

Figure 8. Frequency Spectrum of Pulse Train for $T_p/T = 0.167$ Where $w = 2\pi/T$.

Comparing the S/N input to that of the S/N output of the commutative filter gives the improvement factor, I, of the commutative filter. Since the signal experiences only an insertion loss when passing through the filter, the improvement factor is equal to the noise into the commutative filter, N_i, divided by the noise out of the commutative filter, N_o, and the insertion loss of the commutative filter. The noise out of the commutative filter can be calculated as follows:

$$N_o = \int_{BW} N(f)\, F^2(f)\, df \tag{48}$$

where N(f) is the average power per cycle of the input noise, BW is the bandwidth of the input noise, and F(f) is the frequency response of the commutative filter. The improvement factor for the unloaded case where the effect of the leaky capacitors and the load resistor is neglected is[6]

$$I = \frac{N_i}{N_o} = \left(2Nf_r R_1 C\right)^{1/2} \tag{49}$$

or

$$I_{dB} = 10 \log \left(2Nf_r R_1 C\right) \tag{50}$$

[6]R. Fischl, "Analysis of a Commutated Network," I.E.E.E. Transactions on Aerospace and Navigational Electronics, V. ANE-10, No. 2 (June, 1963), p. 122.

Chapter II

PRACTICAL REALIZATION OF A COMMUTATIVE FILTER

2.1 Filter Design

The filter designed would have to have enough channels so that a pulse train could be passed without undue attenuation. The relation between the frequency at the point where the comb-filter envelope response, $\frac{\sin \frac{n\pi}{N}}{\frac{n\pi}{N}}$, is down 3 decibels to the resonant frequency of the commutative filter, f_r, is

$$f_{3dB} = \frac{N}{2} f_r \tag{51}$$

or

$$N = 2f_{3dB}/f_r \tag{52}$$

If the pulse train in figures 4 and 5 is to be preserved, f_{3dB} should equal at least $4f_r$. Therefore N from equation 52 will equal 8.

The capacitors chosen should have a very low leakage so that the load impedance, R_2, will not be limited to a low value determined by the capacitor leakage. The capacitors chosen were 0.22-microfarad (plus or minus 10 percent) Mylar capacitors. The capacitors were matched to within plus or minus 0.86 percent at a mean value of 0.210 microfarad.

The filter circuit used is shown in figure 9. The logic pulses into this circuit are generated by the logic circuitry in figure 10. The boxes are J-K flip-flops. Motorola MC 790P dual J-K flip-flops were used. The other symbols are for two-input positive logic NOR. Motorola MC 717P quad two-input gates were used. The boxes formed by the dashed lines in figure 10 indicate two integrated-circuit gate packages. A total package count of four integrated-circuit packages resulted. Next to the symbols, the numbers are the package pin numbers, S the set inputs, T the clock inputs, C the clear inputs, C_D the preclear inputs, t_i (where i = 1 to 8) the logic pulses to the transistors in the filter, and the rest of the alphabetic letters are the outputs of the J-K flip-flops. The bar over the letters signifies the opposite state than the same letter with no bar, where there are two states, 0 and 1.

NOTES: 1. ALL C_i ARE 0.21 MICROFARAD
2. ALL Q_i ARE 2N2219

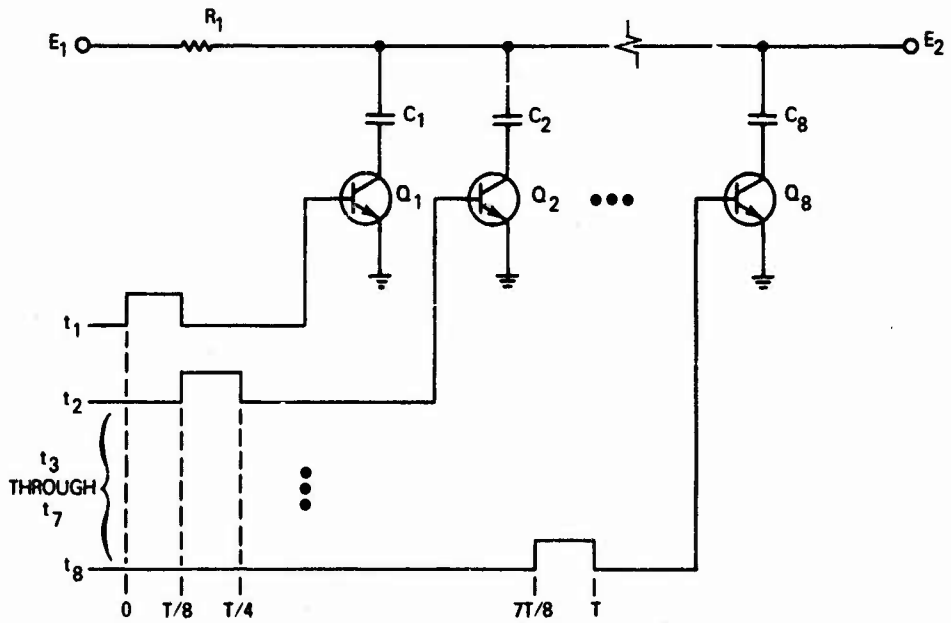

Figure 9. Filter Circuit Diagram.

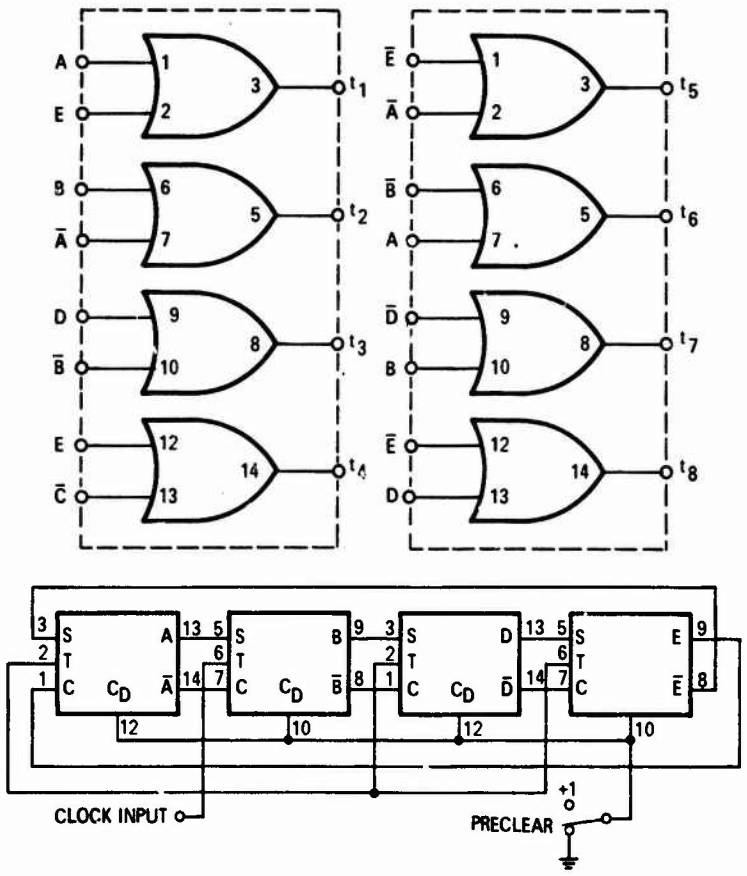

Figure 10. Logic Circuit Diagram.

Figure 11 is the logic waveforms and logic truth table for the logic circuitry. After the flip-flops have been precleared, each clock pulse sets one after another flip-flop until the last flip-flop is set. Then because of the negative feedback to the first flip-flop, the clock pulses will clear one after another flip-flop until the last flip-flop is cleared, at which time the cycle repeats. The truth table shows the output code of the flip-flops and also the outputs that must be specified to determine an output to the commutative filter. The input to the NOR gate is determined from De Morgan's theorem. As an example, the input to the NOR gate necessary to produce t_1 is

$$t_1 = \bar{A}\,\bar{E} = \overline{A + E} \tag{53}$$

Therefore, for the desired output, t_1, the input to the NOR gate must be A and E.

The voltage level of the power supply for the logic should be set to supply enough current to turn the filter transistors on but not load down the gate outputs.

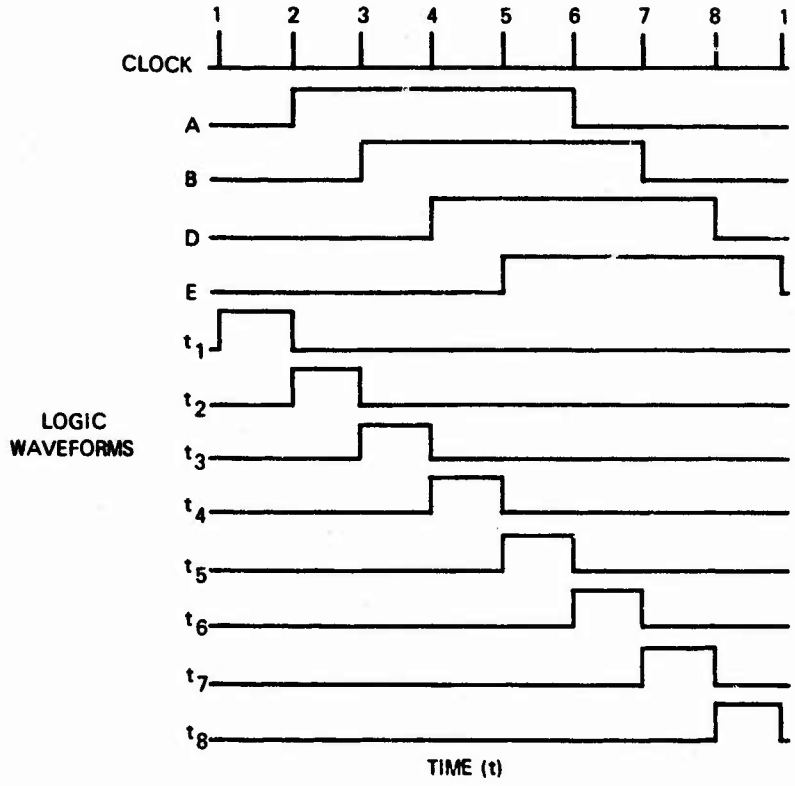

TRUTH TABLE

CLOCK PULSE COUNT	FLIP-FLOP OUTPUT CONDITION E	D	B	A	NECESSARY OUTPUTS TO FILTER
1	0	0	0	0	$\overline{A\bar{E}} = t_1$
2	0	0	0	1	$\bar{B}A = t_2$
3	0	0	1	1	$\bar{D}B = t_3$
4	0	1	1	1	$\bar{E}D = t_4$
5	1	1	1	1	$EA = t_5$
6	1	1	1	0	$B\bar{A} = t_6$
7	1	1	0	0	$D\bar{B} = t_7$
8	1	0	0	0	$E\bar{D} = t_8$

Figure 11. Logic Waveforms and Logic Truth Table.

2.2 Evaluation of Commutative Filter

To check the theory developed in chapter I, the designed filter must be evaluated. Although the filter is constructed from discrete components, the evaluation is applicable to integrated-circuit use.

2.2.1 *Transfer Function Evaluation*

Figure 12 is the block diagram of the test setup used to determine the attenuation at the resonant frequency and its harmonics. The Hewlett-Packard model 3300A function generator was put in the phase-lock mode. In this mode the function generator is capable of producing a sine-wave output that can be phase locked to a pulse input. The output frequency can be set to the input pulse frequency or any of its harmonics up to 110 megahertz. The phase-lock input is from the channel-one output from the logic circuit. The AC amplifier was used as a buffer amplifier. The pulse generator was used to obtain a fast fall time of the clock pulse since a fall time of less than 100 nanoseconds is required for triggering the flip-flops. The output of the Hewlett-Packard model 5245L counter was used as a clock pulse, this output ranging from 0.1 hertz to 10 megahertz in decade steps. Since the resonant frequency of the commutative filter, f_r, is equal to the clock frequency divided by eight (the number of low-pass filter channels). the usable range of f_r is 125 hertz to 125 kilohertz. The lower frequency is limited by the filter bandwidth so that there will be no crossover distortion caused by overlapping bandwidths from the resonant and harmonic frequencies. The upper frequency is limited by the logic response time. The DC power supply for the logic was set at 2.2 volts.

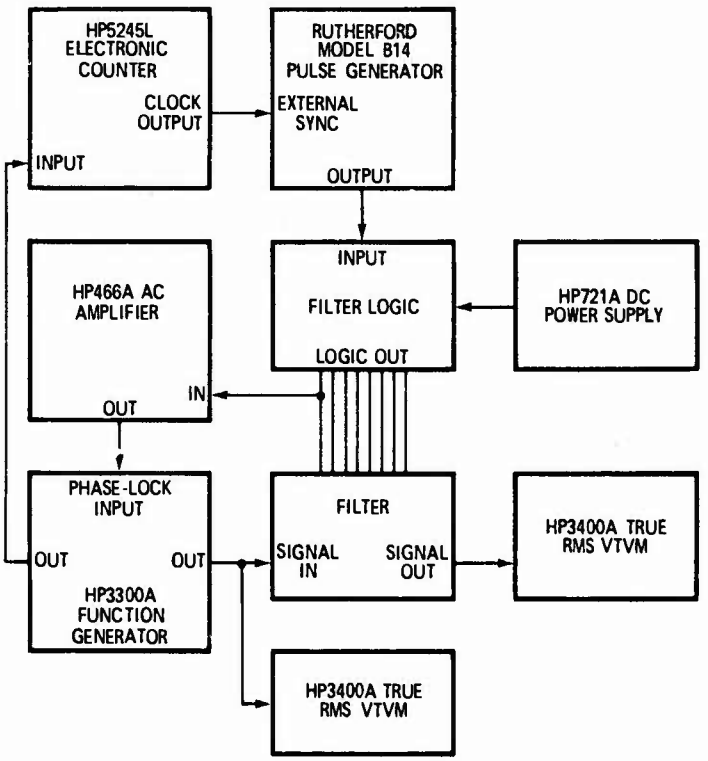

Figure 12. Block Diagram for Determining Attenuation at Resonant and Harmonic Frequencies.

Figure 13 is a plot of the voltage obtained for f_r and the first seven harmonics. The theoretical response is also plotted from the viewpoint of the loading effects. The experimental results are again plotted for the results normalized with respect to the theoretical response at f_r.

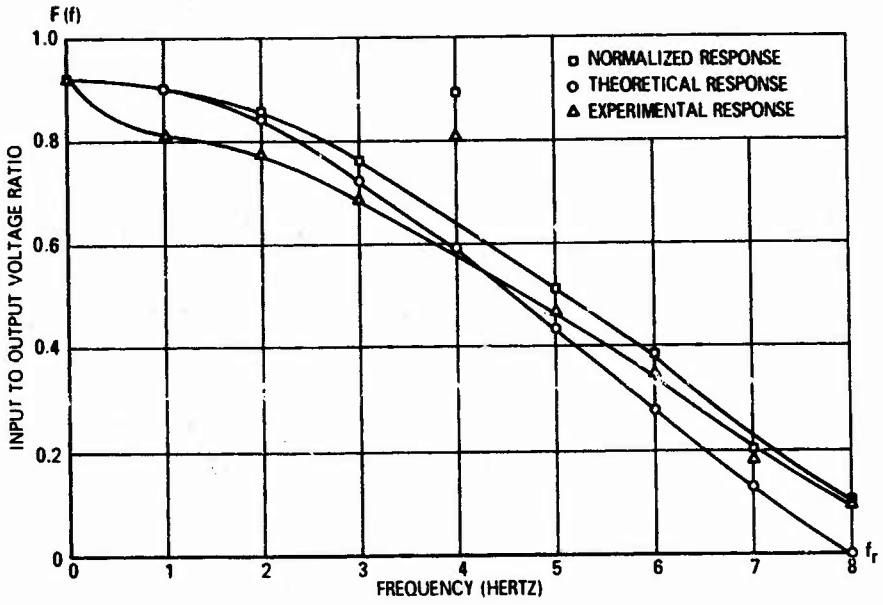

Figure 13. Resonant Frequency and Harmonic Output Response.

Figure 14 is the block diagram used to obtain frequency response curves from the filter. From these curves the experimental transfer function was determined. The function generator is put in the VCO (voltage-controlled oscillator) mode where a voltage ramp of 0 to -10 volts changes the frequency at least one decade with ±1 percent resetability. The schematic diagram of the voltage ramp generator that was used is shown in figure 15. Since the commutative filter operates on the integration principle, where a certain time is required for the capacitors to charge up to the input-sampled voltage, the time rate of increase of the voltage ramp should be as slow as practical. The voltage ramp generator consists of a constant current source charging a capacitor followed by two emitter followers to reduce loading effects.

Figure 16 is a graph obtained for f_r = 12.5 kHz and shows the response of the filter to the resonant frequency and the first seven harmonics.

2.2.2 Bandwidth and Q Evaluation

Frequency response curves about the resonant frequency obtained by using the system described in figure 14 were used to obtain BW measurements, and from these measurements Q was calculated.

Figure 17 is a plot of the center frequency response at f_r = 125 Hz for different values of R_1. Figure 18 is a plot of the resonant frequency response for a resonant frequency of 125, 1,250, and 12,500 hertz. Figure 19 is a plot of the resonant frequency response at a resonant frequency of 125 hertz for variations in the load resistance, R_2. Figure 20 is a plot of the resonant frequency response at a resonant frequency of 125 hertz for variations in the resistor across the capacitor, R_c.

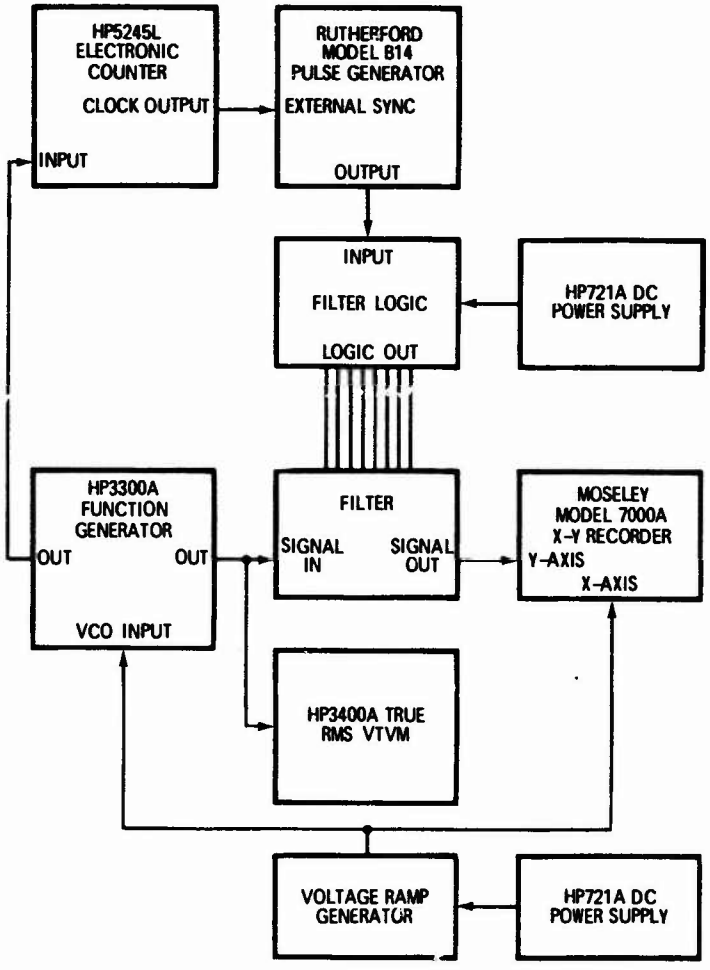

Figure 14. Block Diagram for Obtaining Frequency Plots of the Commutative Filter.

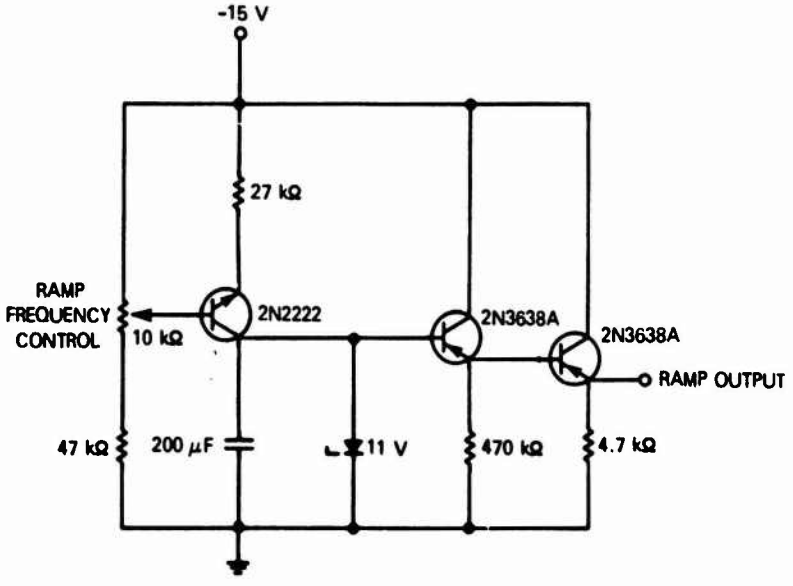

Figure 15. Schematic Diagram for the Voltage Ramp Generator.

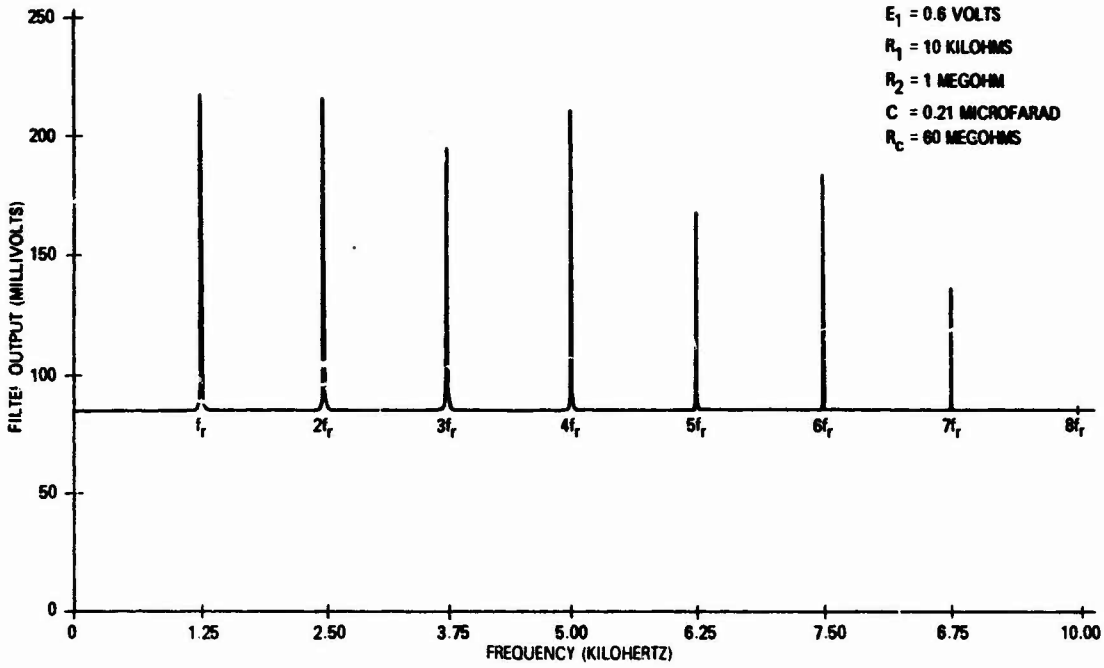

Figure 16. Frequency Response of Commutative Filter at f_r = 1.25 Kilohertz.

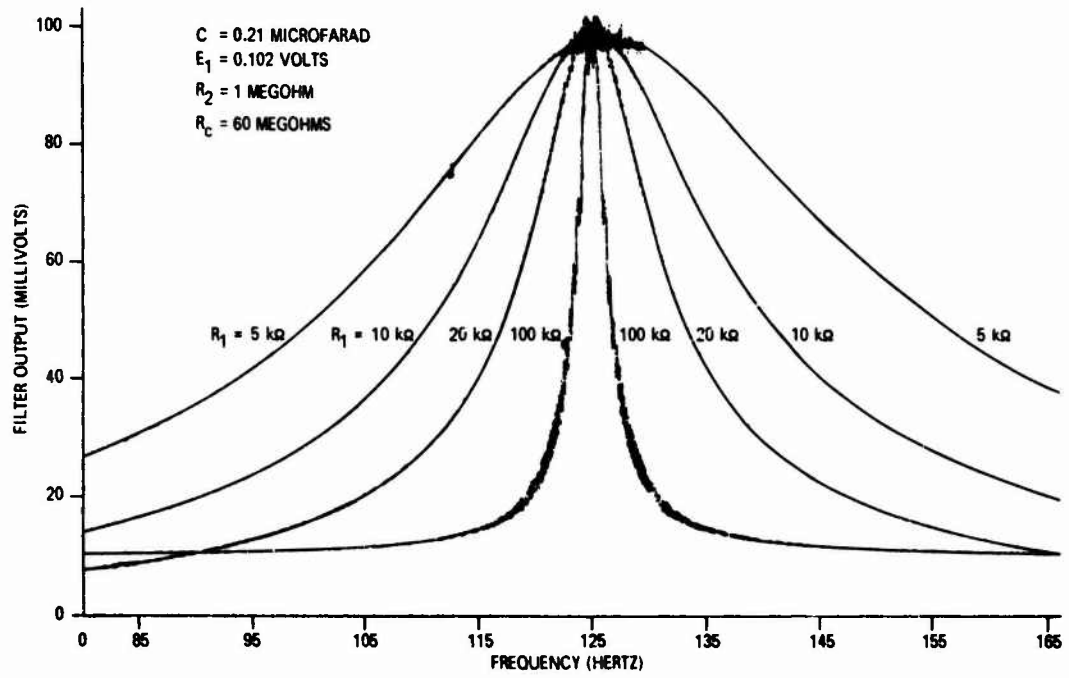

Figure 17. Center Frequency Response at f_r = 125 Hertz.

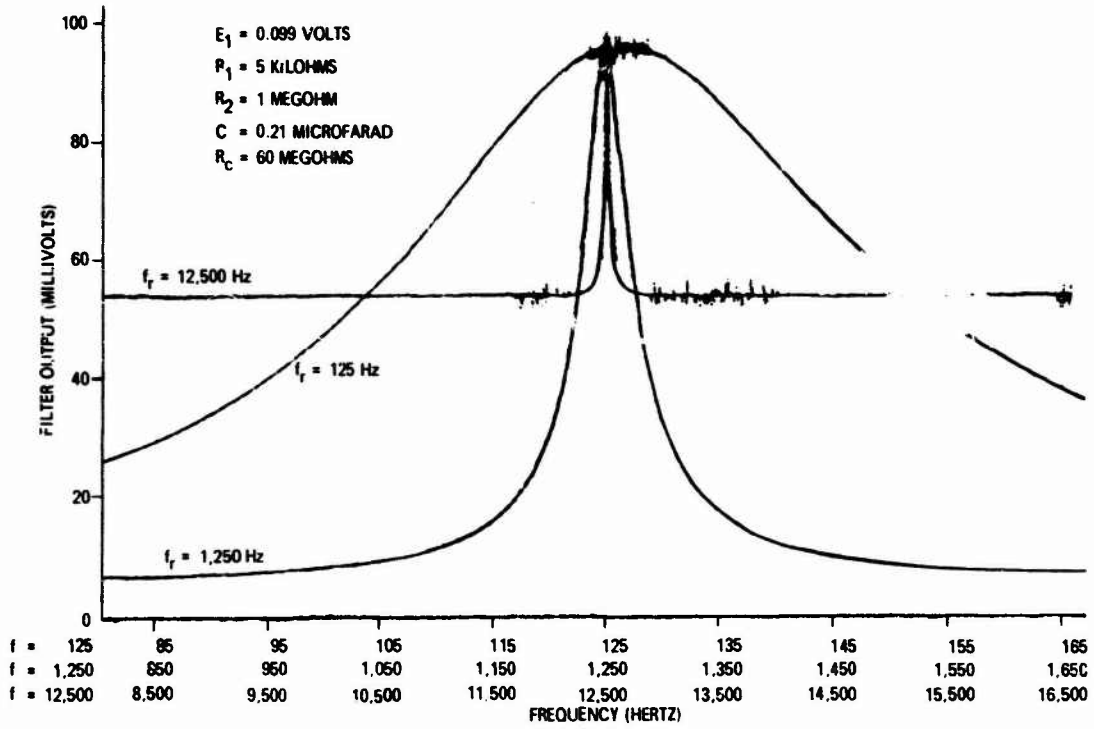

Figure 18. Center Frequency Response With Constant BW for Varied f_r.

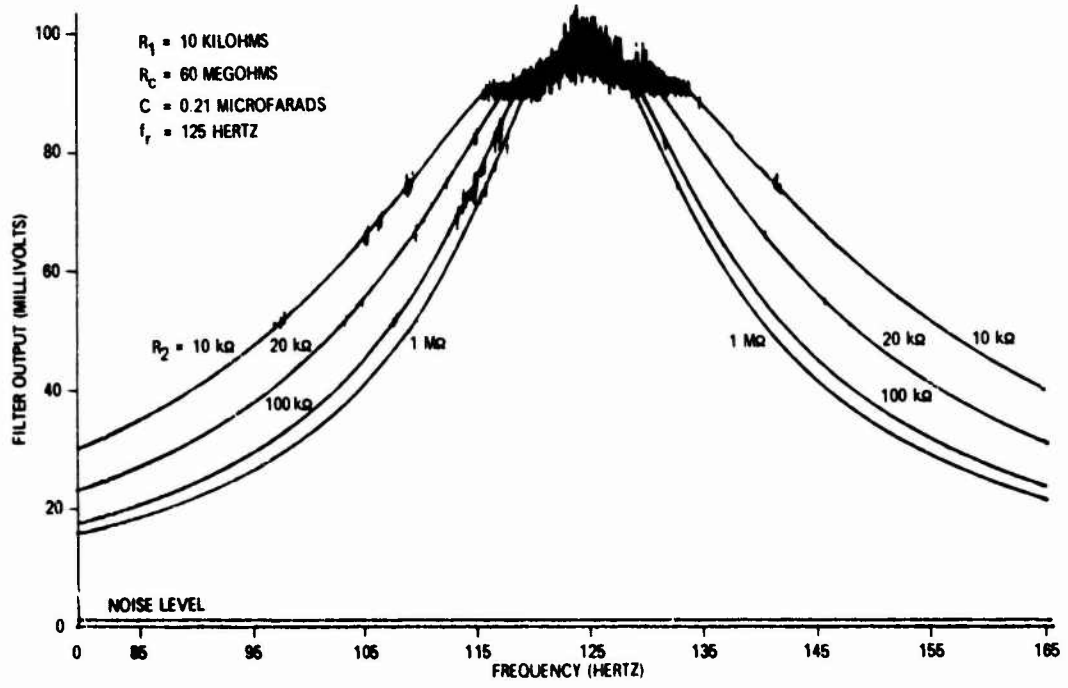

Figure 19. Center Frequency Response When R_2 Is Varied.

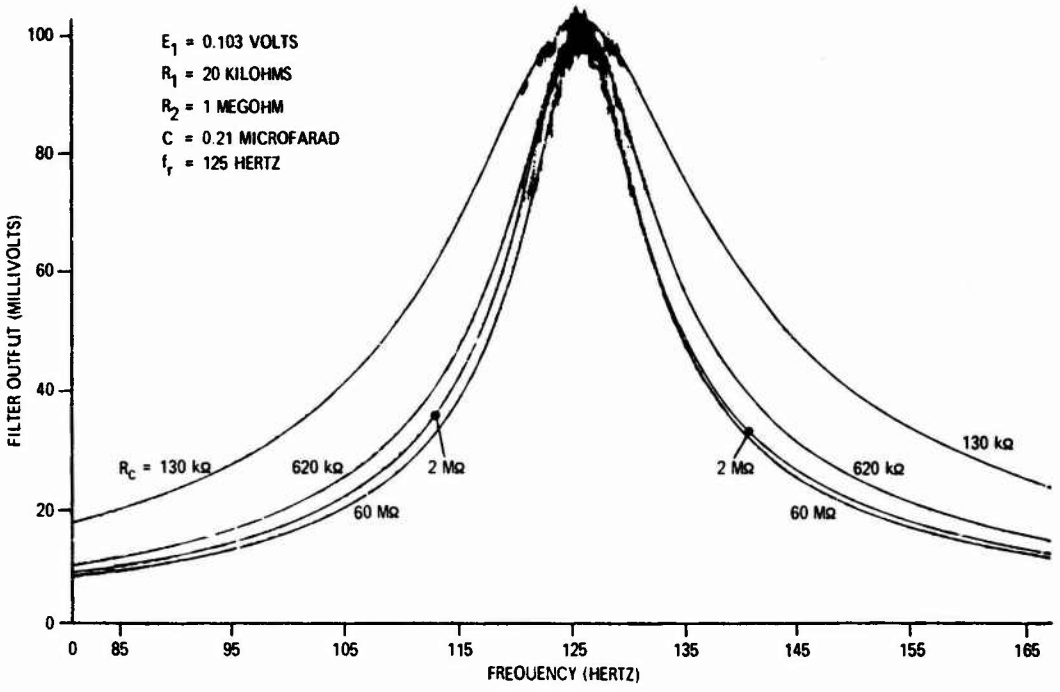

Figure 20. Center Frequency Response for R_C Varied.

2.2.3 Sensitivity Evaluation

The sensitivities of the commutative filter were experimentally determined by measuring the fractional change in one variable caused by a fractional change in an independent variable. The sensitivity factor is then calculated by using equation 28.

Curves for center frequency response were obtained, and commutative filter sensitivities were then calculated from the curves. Table 1 is a tabulation of the sensitivities of the commutative filter versus theoretical values. Figure 21 is a plot of the resonant frequency response at f_r = 125 Hz for small changes in C. Curve 1 is the filter unaltered, C equaling 0.21 microfarads in each channel. For curve 2, a 0.056-microfarad capacitor was added to channels one and two. The same procedure was continued until, for curve 5, all channels had an added 0.056-microfarad capacitance. This capacitance represents a total change in C of 27 percent for the commutative filter, and demonstrates what happens when the channel capacitors are not matched.

Figure 22 shows the sensitivity of the center frequency response to small changes in R_1.

2.2.4 Signal-to-Noise Improvement Evaluation

Figure 23 is the block diagram of the test set used to determine the S/N (signal-to-noise) improvement factor, I. The circuit diagram for the mixer is shown below in figure 24.

Table 2 is a tabulation of calculations necessary to determine the experimental and theoretical values of I.

Table 1. Values of Commutative Filter Sensitivities

Sensitivities	Experimental Values	Calculated Values	
		Load Included	Load Neglected
$S_{R_1}^{BW}$	-1.3	-1.30	-1
$S_{R_2}^{BW}$	-0.39	-0.68	0
$S_{R_c}^{BW}$	-0.30	-0.26	0
S_C^{BW}	-0.92	-1.04	-1
$S_{R_1}^{Q}$	+1.30	+1.30	+1
$S_{R_2}^{Q}$	+0.39	+0.68	0
$S_{R_c}^{Q}$	+0.25	+0.26	0
S_C^{Q}	+0.92	+1.04	+1

For table:

Filter Constants	Filter Component Mean Values
f_r = 125 hertz	R_1 = 10 kilohms
N = 8 channels	R_2 = 1 megohm
	R_c = 2 megohms
	C = 0.21 microfarad

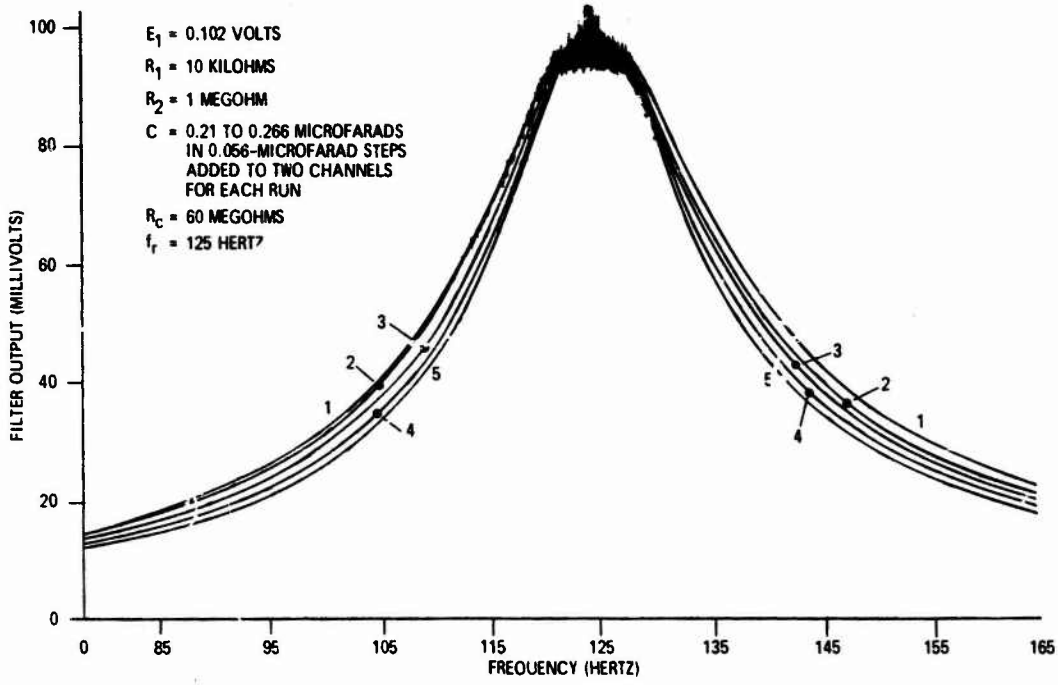

Figure 21. Sensitivity of Center Frequency Response to Small Changes in C.

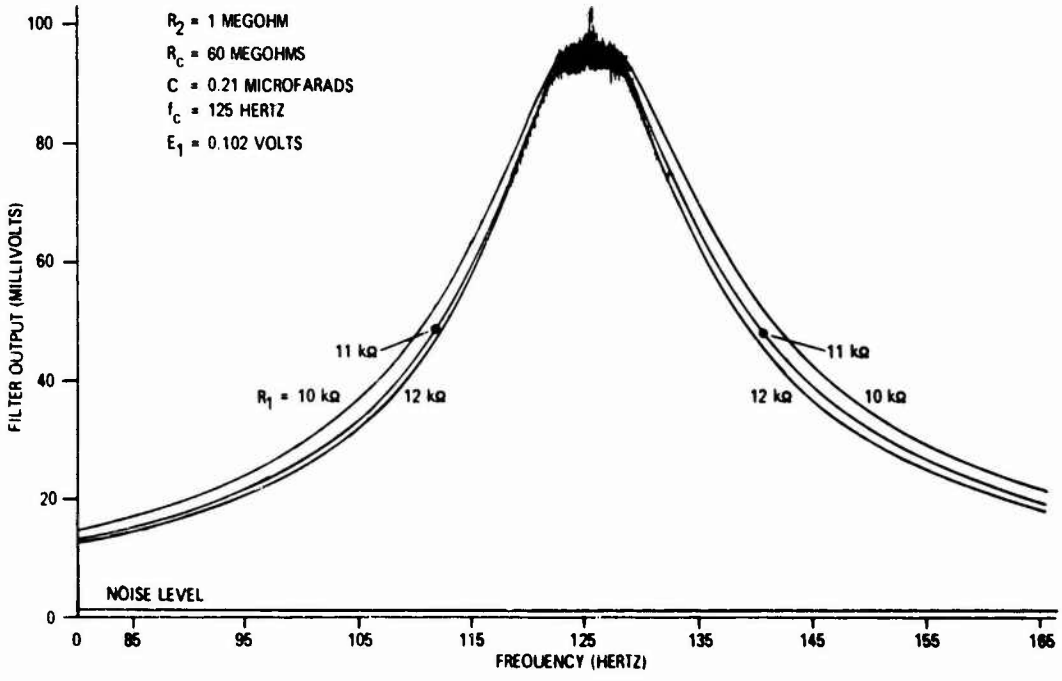

Figure 22. Sensitivity of Center Frequency Response to Small Changes in R_1.

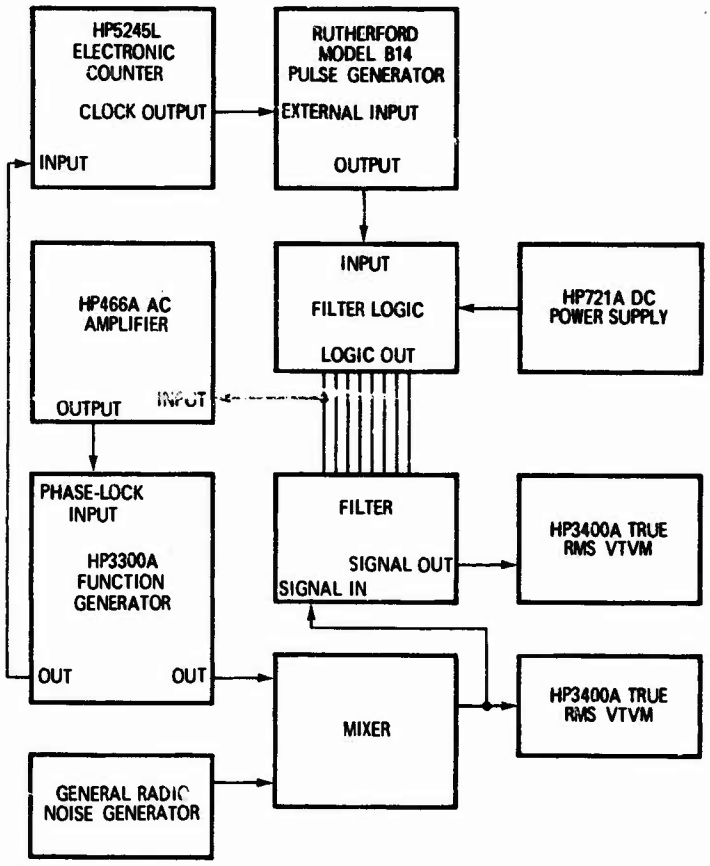

Figure 23. Block Diagram for Obtaining S/N Improvement Factor.

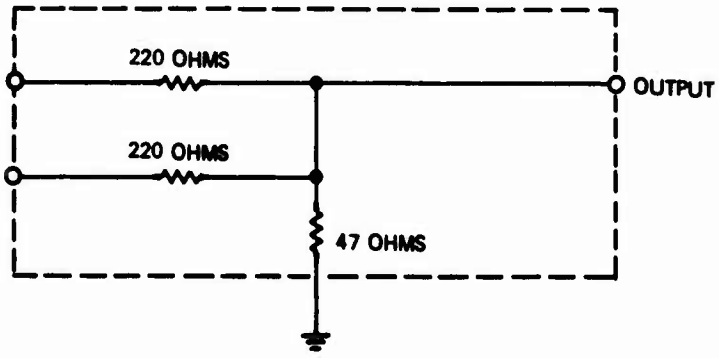

Figure 24. Mixer Circuit Diagram.

Table 2. S/N Improvement Factor, I, of the Commutative Filter

From Theory:	$I_{dB} = 10 \log (2Nf_rR_1C)$	
C	= 0.21 microfarad	0.21 microfarad
N	= 8 channels	8 channels
R_1	= 10 kilohms	20 kilohms
f_r	= 12.5 kilohertz	1.25 kilohertz
I_{dB}	= 26.3 decibels	19.2 decibels
From Experimentation:		
	(Decibels)	(Decibels)
N_i	= -2.5	-2.2
N_o	= -30.7	-28.0
Insertion Loss	= 3.0	3.0
I_{dB}	= 25.2	22.8

where $I_{dB} = N_i - N_0$ - Insertion loss and all values are in decibels.

Chapter III

DISCUSSION OF RESULTS

3.1 Transfer Function

The experimental insertion loss of the filter was 10 percent more than the theoretical value calculated by considering the loading effects. From figure 13 it is seen that the experimental envelope curve matches the calculated envelope curve closely. The noise at the output of the filter is the reason that the output does not go to zero at the eighth harmonic. The normalized curve in figure 13 was obtained by compensating the experimental data by adding to the data the difference in insertion loss at f_r.

3.2 Bandwidth and Q

The experimental values of bandwidths obtained were about 10 percent above the values calculated without consideration of the loading effect and 20 percent below the values calculated with consideration of loading effect. The same correlation was noted for the values of Q. The difference was caused by the fact that the curves were run at a relatively low resonant frequency (125 hertz) so that the frequency responses could be plotted easily. This low frequency yielded a long dwell time so that the range of the ratio of the dwell time to the charge time for the experiment was 0.2 to 0.5. The error then could be calculated from the approximation made to obtain the BW and Q equations. The approximation was

$$e^{-\frac{\text{Dwell Time}}{\text{Charge Time}}} = 1 - \frac{\text{Dwell Time}}{\text{Charge Time}}$$

For the ratio of the dwell time to the charge time of 0.5

$$e^{-0.5} = 0.607$$

and $1 - (.5) = 0.5$

The error in the approximation was 16.5 percent. Therefore if the values calculated with consideration of the loading effects were compensated by the error in the approximation, the values would have been in very close agreement with the experimentally obtained data.

The noise shown on top of the center frequency response curves (figures 17, 18, 19, 20, 21, 22) was due to the resonant frequency (from the sampling action) beating with the input frequency to produce a difference frequency that shows up on the output as oscillations. These oscillations could have been removed by postfiltering, but it was felt that the exact response of the filter would be of more interest.

3.3 Sensitivity

There was a reasonably close correlation between the experimentally obtained values and the calculated values (both including and not including the loading). The sensitivities of BW and Q were low for R_2 and R_c, as was expected by the zero sensitivity calculated for not including the loading.

3.4 Signal-to-Noise Improvement

The biggest problem with the commutative filter in signal-to-noise ratio improvement is that the filter itself adds noise, switching noise caused by the unequal saturation voltages of the transistor switches, unequal stored charge on the capacitors, and feed-through spikes from the logic input. So the improvement that can be gained has its limitations. For large enough signal voltages and large noise power, however, it is seen from table 2 that the calculated and theoretical values of I, the improvement factor, are closely similar.

Chapter IV

CONCLUSION

It has been found that the performance of a practical bandpass commutative filter, one with "leaky capacitors" and a load resistor, is close to theoretical predictions. The testing has also reemphasized the facts that the resonant frequency of the filter can be changed easily (simply by changing the clock frequency) and also that the bandwidth can be changed easily (simply by using a potentiometer for R_1 and varying this potentiometer will give a directly proportional change in the bandwidth).

Other advantages of the filter have been demonstrated, such as the comb-filter response, which can yield a significant signal-to-noise improvement in a postdetector in a radar or communications gear. The comb-filter response can be a disadvantage if not all of the harmonic outputs of the filter resonant frequency are wanted (including the zeroth harmonic, the lowpass response). For this reason low-Q bandpass prefiltering is sometimes needed. Since the output is in the form of the sampled input, there is a postfiltering requirement if it is necessary for closer reshaping of the output waveform to resemble the input waveform.

The most inspiring advantage is that the whole commutative filter, including logic, can be integrated. The author had a chance to examine a three-channel commutative filter completely integrated on a one-inch by three-quarters-inch chip. Exact details were withheld because of the classified application of the filter.

BIBLIOGRAPHY

Chang, David Kuan, Analysis of Linear Systems, Reading, Massachusetts: Addison-Wesley Publishing Company, Inc., 1959.

Dabrowa, A.R., "Analysis of Commutater Filter," U.C.L.A. Master of Science in Engineering Thesis, 1967.

Franks, L.E. and I.W. Sandberg, "An Alternate Approach to the Realization of Network Transfer Functions: the N-path Filter," Bell System Technical Journal, V. 39, No. 5 (September, 1960), pp. 1321-1350.

Franks, L.E. and Witt, F.J., "Solid-State Sampled-Data Bandpass Filters," 1960 International Solid-State Circuits Conference, February, 1960, pp. 70-71.

Fischl, R., "Analysis of a Commutated Network," I.E.E.E. Transactions on Aerospace and Navigational Electronics, V. ANE-10, No. 2 (June, 1963), pp. 114-123.

Harden, William R., "Digital Filters with IC's Boost Q Without Inductors," Electronics V. 40, No. 15 (24 July 1967), pp. 91-100.

Kaufman, M.A., "Theory and Synthesis of the Digitalized Bandpass Filter," U.C.L.A. Master of Science in Engineering Thesis, 1966.

Le Page, W.R., Cahn, C.R., and Brown, J.S., "Analysis of a Comb Filter Using Synchronously Commutated Capacitors," A.I.E.E. Transactions, V. 72, pt. 1 (Communications and Electronics) No. 5 (March, 1953), pp. 63-68.

Smith, B.D., "Analysis of Commutated Networks," I.R.E. Transactions on Aeronautical and Navigational Electronics, No. PGAE-10 (December, 1953), pp. 21-26.

Thompson, James, "RC Digital Filter for Microcircuit Bandpass Amplifiers," Electronic Equipment Engineering, V. 108 (March, 1964), pp. 45-49.